

Evaluation of HLbB contributions to the muon anomalous magnetic moment using holographic QCD

Luigi Cappiello

Dipartimento di Fisica “Ettore Pancini”, Università di Napoli “Federico II”
and
INFN-Sezione di Napoli, Italy

based on

- ▶ L.C. , O. Catá, G. D’Ambrosio, D. Greynat, A. Iyer
Axial-vector and pseudoscalar mesons in the hadronic light-by-light contribution to the muon $(g - 2)$, Phys.Rev.D 102 (2020) 1, 016009, (1912.02779 [hep-ph])
- ▶ L.C. , O. Catá, G. D’Ambrosio
Scalar resonances in the hadronic light-by-light contribution to the muon $(g-2)$, Phys.Rev.D 105 (2022) 5, 056020, (2110.05962 [hep-ph])

Outline

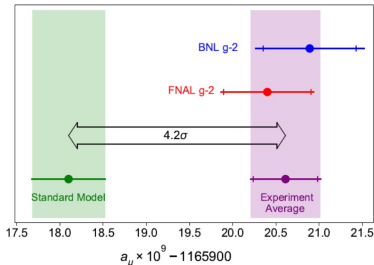
- ▶ Theory vs experiment after the '21 Fermilab measurement of a_μ
- ▶ The hadronic light-by-light contribution
 - ▶ The HLbL tensor
 - ▶ The master formula for a_μ^{HLbL}
 - ▶ One-pion exchange contribution
- ▶ Evaluating the HLbL contribution with HQCD models
 - ▶ HQCD models: ingredients and recipe
 - ▶ The pion transition form factor from HQCD
- ▶ Vector and axial-vector contributions to HLbL
 - ▶ Fulfilling pQCD short distance constraints
 - ▶ Assessing SD contributions to HLbL
- ▶ Further contributions to HLbL: scalars in HQCD models
- ▶ Conclusions

Theory vs experiment after the Fermilab measurement

The 2021 Fermilab experiment result combined with the previous E821 result has enlarged the discrepancy between experimental and theoretical (SM) values of $a_\mu = (g - 2)_\mu/2$ from 3.7σ to 4.2σ

Status before Fermilab(21)

Contribution	Value $\times 10^{11}$	Combined Exp(21) $116592061(41) \times 10^{11}$
Experiment (E821)	116 592 089(63)	
HVP LO (e^+e^-)	6931(40)	
HVP NLO (e^+e^-)	-98.3(7)	
HVP NNLO (e^+e^-)	12.4(1)	
HVP LO (lattice, $udsc$)	7116(184)	
HLbL (phenomenology)	92(19)	
HLbL NLO (phenomenology)	2(1)	
HLbL (lattice, uds)	79(35)	
HLbL (phenomenology + lattice)	90(17)	
QED	116 584 718.931(104)	
Electroweak	153.6(1.0)	
HVP (e^+e^- , LO + NLO + NNLO)	6845(40)	
HLbL (phenomenology + lattice + NLO)	92(18)	
Total SM Value	116 591 810(43)	



Current status of experiment and SM theoretical predictions for a_μ ([Muon g-2 collaboration PRL 126 \(21\) 14181](#)). The theoretical prediction is taken from the [White Paper \(Ayoama et. al. Phys.Rept 887 \(20\) 1-166\)](#)

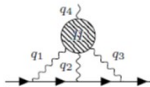
Hadronic contributions to a_μ

Hadronic Vacuum Polarization (HVP) and Hadronic Light-by-Light scattering (HLbL).
 HVP related through unitarity cut to physical $e^+ - e^-$ cross section.
 Only recently dispersion techniques systematically applied to HLbL (data driven approach), previous estimates based on phenomenological models

HVP and HLbL Feynman diagrams



HVP contribution to $g - 2$



HLbL contribution to $g - 2$

Evolution of the theoretical estimates of the various processes contributing to HLbL

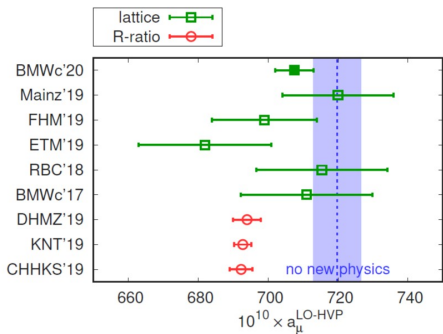
Contribution	PdRV(09)	N/JN(09)	J(17)	WP(20)
π^0, η, η' -poles	114(13)	99(16)	95.45(12.40)	93.8(4.0)
π, K -loops/boxes	-19(19)	-19(13)	-20(5)	-16.4(2)
S -wave $\pi\pi$ rescattering	-7(7)	-7(2)	-5.98(1.20)	-8(1)
subtotal	88(24)	73(21)	69.5(13.4)	69.4(4.1)
scalars	-	-	-	} -1(3)
tensors	-	-	1.1(1)	
axial vectors	15(10)	22(5)	7.55(2.71)	
u, d, s -loops / short-distance	-	21(3)	20(4)	15(10)
c -loop	2.3	-	2.3(2)	3(1)
total	105(26)	116(39)	100.4(28.2)	92(19)

- ▶ HLbL major source of uncertainty to the hadronic contributions to a_μ , and a lot of effort (and progress) has been done very recently to assess its value.
- ▶ Recently, lattice collaborations have published values for HVP which greatly differ with previous estimates and would push the total value of a_μ close to the experimental value. It was a bolt in clear sky, currently under scrutiny.

Theoretical conundrum on HVP

Data driven approach based on unitarity and R-ratio evaluation and Lattice QCD results give "incompatible" results. Here are BMW collaboration result and more recent (june '22) investigations

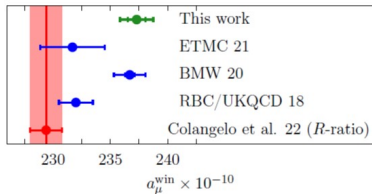
HVP contributions according to BMWc'20 paper



Lattice (green squares), R-ratio method (data driven approach) (red circles)

A very recent (june 22) compilation of HVP estimates (in a particular Euclidean window)

A.Ce' et al arXiv:2206.06582



Lattice QCD: green point A.Ce' et al (22) and blue points. Red point data driven analysis of G.Colangelo et al. 2205.12963 [hep-ph]

The Hadronic Light-by-Light Tensor

$$\Pi^{\mu\nu\lambda\sigma}(q_1, q_2, q_3) = -i \int d^4x d^4y d^4z e^{-i(q_1 \cdot x + q_2 \cdot y + q_3 \cdot z)} \langle |T\{j_{\text{em}}^\mu(x) j_{\text{em}}^\nu(y) j_{\text{em}}^\lambda(z) j_{\text{em}}^\sigma(0)\}| \rangle$$

$$q_4 = q_1 + q_2 + q_3$$

138 Lorentz structures

$$\begin{aligned} \Pi^{\mu\nu\lambda\sigma} &= g^{\mu\nu} g^{\lambda\sigma} \Pi^1 + g^{\mu\lambda} g^{\nu\sigma} \Pi^2 + g^{\mu\sigma} g^{\nu\lambda} \Pi^3 \\ &+ \sum_{i,j=1,2,3} \left(g^{\mu\nu} q_i^\lambda q_j^\sigma \Pi_{ij}^4 + g^{\mu\lambda} q_i^\nu q_j^\sigma \Pi_{ij}^5 + g^{\mu\sigma} q_i^\nu q_j^\lambda \Pi_{ij}^6 \right. \\ &+ \left. g^{\nu\lambda} q_i^\mu q_j^\sigma \Pi_{ij}^7 + g^{\nu\sigma} q_i^\mu q_j^\lambda \Pi_{ij}^8 + g^{\lambda\sigma} q_i^\mu q_j^\nu \Pi_{ij}^9 \right) \\ &+ \sum_{i,j,k,l=1,2,3} q_i^\mu q_j^\nu q_k^\lambda q_l^\sigma \Pi_{ijkl}^{10} \end{aligned}$$

95 linearly independent relations

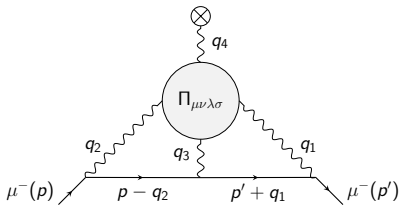
from gauge invariance \implies

$$\{q_{1\mu}, q_{2\nu}, q_{3\rho}, q_{4\sigma}\} \Pi^{\mu\nu\lambda\sigma}(q_1, q_2, q_3) = 0$$

Complete crossing symmetric

$$C_{14} = \{q_1 \leftrightarrow -q_4, \mu \leftrightarrow \sigma\}, \quad C_{13} = \{q_1 \leftrightarrow q_3, \mu \leftrightarrow \lambda\}$$

The HLbL tensor in the HLbL diagram



43 linearly independent tensor structures

BTT basis: 54 (redundant) tensor structures, with scalar functions Π_i free of kinematic singularities [Colangelo et al.\(15\)](#)

$$\Pi^{\mu\nu\lambda\sigma} = \sum_{i=1}^{54} T_i^{\mu\nu\lambda\sigma} \Pi_i,$$

Master Formula for a_{μ}^{HLbL}

$$\begin{aligned}
 a_{\mu}^{\text{HLbL}} = & -\frac{e^6}{48m_{\mu}} \int \frac{d^4 q_1}{(2\pi)^4} \frac{d^4 q_2}{(2\pi)^4} \frac{1}{q_1^2 q_2^2 (q_1 + q_2)^2} \frac{1}{(p + q_1)^2 - m_{\mu}^2} \frac{1}{(p - q_2)^2 - m_{\mu}^2} \\
 & \times \text{Tr} \left((\not{p} + m_{\mu}) [\gamma^{\rho}, \gamma^{\sigma}] (\not{p} + m_{\mu}) \gamma^{\mu} (\not{p} + \not{q}_1 + m_{\mu}) \gamma^{\lambda} (\not{p} - \not{q}_2 + m_{\mu}) \gamma^{\nu} \right) \\
 & \times \sum_{i=1}^{54} \left(\frac{\partial}{\partial q_4^{\rho}} T_{\mu\nu\lambda\sigma}^i(q_1, q_2, q_4 - q_1 - q_2) \right) \Big|_{q_4=0} \bar{\Pi}_i(q_1, q_2, -q_1 - q_2).
 \end{aligned}$$

Only 19 independent linear combinations of the 54 $T_i^{\mu\nu\rho\lambda}$ contribute to a_{μ}^{HLbL} . Using Gegenbauer polynomials techniques (Knecht Nyffeler (01)), the symmetry of the loop integral and the propagators, there remain 12 different integrals containing 12 coefficients $\bar{\Pi}_i(q_1, q_2, -q_1 - q_2)$.

$$a_{\mu}^{\text{HLbL}} = \frac{2\alpha^3}{3\pi^2} \int_0^{\infty} dQ_1 \int_0^{\infty} dQ_2 \int_{-1}^1 d\tau \sqrt{1 - \tau^2} Q_1^3 Q_2^3 \sum_{i=1}^{12} \bar{T}_i(Q_1, Q_2, \tau) \bar{\Pi}_i(Q_1, Q_2, \tau),$$

where $Q_1 := |Q_1|$, $Q_2 := |Q_2|$. $\bar{\Pi}_i$ evaluated for the reduced kinematics

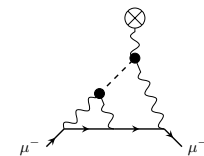
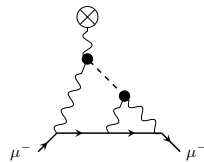
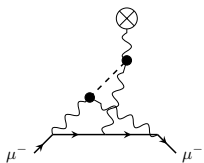
$$q_1^2 = -Q_1^2, \quad q_2^2 = -Q_2^2, \quad q_3^2 = -Q_3^2 = -Q_1^2 - 2Q_1 Q_2 \tau - Q_2^2, \quad q_4^2 = 0.$$

Integral kernels expressions $\bar{T}_i(Q_1, Q_2, \tau)$, in Colangelo et al.(15&17)

TFF and one-pion exchange HLbL diagrams

Leading contribution in the Large- N_c and chiral limit

HLbL One-pion exchange diagrams.



Ansätze für $\mathcal{F}_{P\gamma^*\gamma^*}(q_1^2, q_2^2)$

$$\text{WZW} : - \frac{N_c}{12\pi^2 f_\pi}$$

$$\text{VMD} : - \frac{N_c}{12\pi^2 f_\pi} \frac{m_V^2}{(q_1^2 - m_V^2)} \frac{m_V^2}{(q_2^2 - m_V^2)}$$

$$\text{LMD} : \frac{f_\pi}{3} \frac{q_1^2 + q_2^2 - (N_c m_V^4 / (4\pi^2 f_\pi^2))}{(q_1^2 - m_V^2)(q_2^2 - m_V^2)}$$

$$\text{LMD} + V : \frac{f_\pi}{3} \frac{P_6(q_1^2, q_2^2, M_{V_1}^2, M_{V_2}^2; h_1, h_2, h_5)}{(q_1^2 - m_{V_1}^2)(q_2^2 - m_{V_1}^2)(q_1^2 - m_{V_2}^2)(q_2^2 - m_{V_2}^2)}$$

Knecht, Nyffeler(01)

$$\text{DIP} : - \frac{N_c}{12\pi^2 f_\pi} \left(1 + \lambda \left(\frac{q_1^2}{(q_1^2 - m_{V_1}^2)} + \frac{q_2^2}{(q_2^2 - m_{V_2}^2)} \right) \right)$$

$$+ \eta \sum_{i=1,2} \frac{q_1^2 q_2^2}{(q_1^2 - m_{V_i}^2)(q_2^2 - m_{V_i}^2)} \quad \text{C, Cata, D'Ambrosio(11)}$$

$a_{\mu}^{\text{HLbL},\pi^0}$ estimates

$a_{\mu}^{\text{HLbL},\pi^0} \times 10^{-9}$		
VMD	5.7	KN(01)
LMD+V	6.3	KN(01)
DIP	6.58	CCD(11)
$\langle \text{HQCD's} \rangle$	5.9(2)	LMR(19)
DVR interp.	5.64(25)	DVR(19)
Lattice	5.97 ± 0.23	GMN(19)

$\langle \text{HQCD's} \rangle$ LMR(19) $a_{\mu}^{\text{HLbL},\pi^0} \times 10^{-9}$	
SS	4.83
HW1	6.13
HW2	5.66
SW	5.92

Danilkin, Redmer, Vandraeghen(19), Gérardin, Meyer, Nyffeler(19)

DIP refers to an “Hybrid” HQCD approach of C, Cata, D’Ambrosio (11), updated and extended by Leutgelb, Mager and Rebhan (19)

Holographic QCD

Good features

- ▶ Lagrangian formulation (although in 5D)
- ▶ Leading Short Distance (SD) from pQCD reproduced by HQCD models with (asymptotic) 5D AdS metric
- ▶ In AdS slice (IR cut-off) (Hard-Wall models) or with also quadratic dilaton background (Soft-Wall models), there are an infinite number of (KK) resonances saturating the channels as expected for Large- N_c QCD
- ▶ Small number of free parameters (e.g. 5D gauge coupling and size of the extradimension)
- ▶ Many explicit analytic calculations

Not-so-good features

- ▶ χ SB realized in different ways (but we have our favourite model!)
- ▶ Different kind of resonances mass spectra (Regge vs non Regge)
- ▶ One top-down approach (Sakai-Sugimoto) not even asymptotically AdS, but giving reasonable low-energy hadronic physics

Holographic models of QCD

SS: Sakai,Sugimoto(05)

HW1: Erlich, Katz, Son, Stephanov(05) ,Da Rold, Pomarol(05)

HW2: Hirn,Sanz(05)

SW: Karch, Katz, Son, Stephanov(06)

... and many descendants

Holographic models of QCD: ingredients & recipes

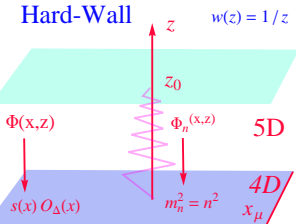
HQCD models inspired by AdS/CFT duality between a 4D (conformal) (Large- N_c) gauge theory at strong coupling and a (classical) 5D field theory in a curved Anti-de Sitter space

$$\exp(iW[s(\mathbf{x})]) \equiv \left\langle \exp \left(i \int d^4x \mathbf{s}(\mathbf{x}) O_\Delta(x) \right) \right\rangle_{QCD} = \exp(i S_5(\Phi_0(z, \mathbf{x})))$$

Maldacena (97), Gubser Klebanov Polyakov (98), Witten (98)

Hard-Wall

$$w(z) = 1/z$$



4D

operator $O_\Delta(x)$
source $\mathbf{s}(\mathbf{x})$ coupled to $O_\Delta(x)$
conformal dimension Δ

$U(N_f)_L \times U(N_f)_R$

global symmetry

vector current $\bar{q} \gamma^\mu t^a q$ $\mathbf{v}_\mu^a(\mathbf{x}) \leftarrow$

axial current $\bar{q} \gamma^\mu \gamma_5 t^a q$ $\mathbf{a}_\mu^a(\mathbf{x}) \leftarrow$

quark bilinear $\bar{q} t^a q$ $\mathbf{s}(\mathbf{x}) \leftarrow$

5D

dual field $\Phi(x, z)$

on-shell $\Phi_0(x, z) \rightarrow \mathbf{s}(\mathbf{x})$

mass m_Φ :

$$m_\Phi^2 = (\Delta - p)(\Delta + p - 4)$$

$U(N_f)_L \times U(N_f)_R$

gauge symmetry

gauge field $V_\mu^a(x, z)$

gauge field $A_\mu^a(x, z)$

scalar field $X^a(x, z)$

confinement

Hard-Wall: sharp cut-off $0 \leq z \leq z_0$

Soft-Wall: dilaton potential

Chiral Symmetry Breaking

5D profile $X(z)$

5D parity/ ChSB boundary conditions

(Large- N_c) QCD correlators from *on-shell* S_5

- ▶ 2-point Functions: VV, AA and SS Current-Current Correlators

$$\langle 0 | T \{ J_V^\mu(x) J_V^\nu(y) \} | 0 \rangle \iff \frac{\delta^2 S_5}{\delta v^\mu(x) \delta v^\nu(y)}$$

$$\langle 0 | T \{ J_A^\mu(x) J_A^\nu(y) \} | 0 \rangle \iff \frac{\delta^2 S_5}{\delta a^\mu(x) \delta a^\nu(y)}$$

$$\langle 0 | T \{ J_S(x) J_S(y) \} | 0 \rangle \iff \frac{\delta^2 S_5}{\delta s(x) \delta s(y)}$$

- ▶ 3-point Functions: The Pion Transition Form Factor

$$\langle \pi(x) | T \{ J_{e.m.}^\mu(y) J_{e.m.}^\nu(z) \} | 0 \rangle \iff \frac{\delta^3 S_5}{\delta \pi(x) \delta v_0^\mu(y) \delta v_0^\nu(z)}$$

- ▶ 4-point Function: The Hadronic Light-by-Light Tensor

$$\begin{aligned} & \langle 0 | T \{ J_{e.m.}^\mu(x) J_{e.m.}^\nu(y) J_{e.m.}^\lambda(z) J_{e.m.}^\sigma(w) \} | 0 \rangle \\ & \iff \frac{\delta^4 S_5}{\delta v_0^\mu(x) \delta v_0^\nu(y) \delta v_0^\lambda(z) \delta v_0^\sigma(w)} \end{aligned}$$

HQCD: *minimal* 5D Lagrangian

$$S_5 = \int d^5x \sqrt{g} (\mathcal{L}_{\text{YM}} + \mathcal{L}_X) + S_{CS}$$

$$\mathcal{L}_{\text{YM}} = -\lambda \text{tr} \left[F_{(L)}^{MN} F_{(L)MN} + F_{(R)}^{MN} F_{(R)MN} \right] \quad \mathcal{L}_X = \rho \text{tr} \left[D^M X^\dagger D_M X - m_X^2 X^\dagger X \right]$$

$$S_{CS} = \int \text{tr} [\omega_5(L) - \omega_5(R)]$$

- ▶ AdS_5 metric $ds_5^2 = \frac{1}{z^2} (dx_\mu^2 - dz^2)$. $0 \leq z \leq z_0$, with $z_0 \propto 1/m_\rho$
- ▶ X transforms as a bifundamental of $U(3)_L \times U(3)_R$: $X \rightarrow g_L X g_R^\dagger$
- ▶ $\mathcal{F}_{MN} = \partial_M \mathcal{A}_N - \partial_N \mathcal{A}_M - i[\mathcal{A}_M, \mathcal{A}_N]$ and $\mathcal{A}_{L,R} = V \mp A$,
- ▶ In the HW1 models the 5D scalar field $X(x, z)$, dual to $\bar{q}q$, induces χSB , by acquiring a non trivial 5D profile $X = X_0(z)$
- ▶ In HW2 there is no 5D scalar field. χSB broken by different boundary conditions for V_μ and A_μ on the IR wall z_0 and the **4D chiral field $U(x)$ appears in the zero mode part of $A_\mu(x, z)$.**
- ▶ The Chern-Simons S_{CS} term describes anomalous processes

3-point Function: Pion TFF from HW2

$$\int d^4x e^{-iq_1 \cdot x} \langle P(q_1 + q_2) | T \{ J_{e.m.}^\mu(x) J_{e.m.}^\nu(0) \} | \rangle = \epsilon^{\mu\nu\rho\sigma} q_{1\rho} q_{2\sigma} \mathcal{F}_{P\gamma^*\gamma^*}(Q_1^2, Q_2^2)$$

where $Q_{1,2}^2 = -q_{1,2}^2$

For $P = \pi^0$, real photons normalization

$$\mathcal{F}_{\pi^0\gamma^*\gamma^*}(0, 0) = \frac{N_c}{12\pi^2 f_\pi} \quad (\text{pointlike WZW vertex})$$

Normalized TFF $K(Q_1^2, Q_2^2) \equiv \mathcal{F}_{P\gamma^*\gamma^*}(Q_1^2, Q_2^2) / \mathcal{F}_{P\gamma^*\gamma^*}(0, 0) \rightarrow K(0, 0) = 1$

Where is the pion field in HW2?

$$V_\mu(x, z) = v_\mu(x) + V_\mu^{(reson)}(x, z)$$
$$A_\mu(x, z) = \left(a_\mu(x) + \frac{\partial_\mu \pi(x)}{f_\pi} \right) \alpha(z) + A_\mu^{(reson)}(x, z)$$

Anomalous AVV amplitudes from trilinear terms in the CS action

$$S_{CS}^{(3)} = \frac{N_c}{24\pi^2} \int \text{tr} \left(L(dL)^2 - R(dR)^2 \right) \quad \text{with } L = V + A, R = V - A$$

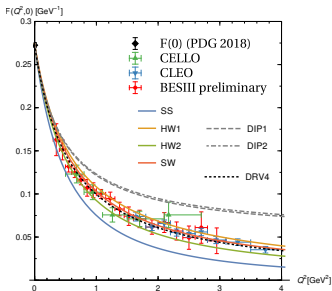
3-point Functions: The Pion Transition Form Factor

$$K(Q_1^2, Q_2^2) = - \int_0^{z_0} v(Q_1, z)v(Q_2, z)\partial_z\alpha(z)dz \quad \Rightarrow \quad \text{---} \bullet \begin{array}{l} \diagup \\ \diagdown \end{array}$$

$v(q^2, z)$: vector bulk-to-boundary propagator, α : pion “wave function”

Low- Q^2

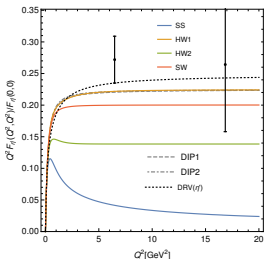
$$K(Q_1^2, Q_2^2) = 1 + \hat{\alpha}(Q_1^2 + Q_2^2) + \hat{\beta} Q_1^2 Q_2^2 + \hat{\gamma}(Q_1^4 + Q_2^4) + \dots$$



Short distance $Q^2 \gg \Lambda_{QCD}$

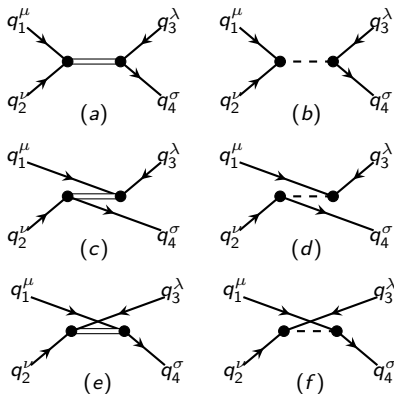
$$K^{pQCD}(Q^2, 0) = \frac{8\pi^2 f_\pi^2}{Q^2}$$

$$K^{pQCD}(Q^2, Q^2) = \frac{8\pi^2 f_\pi^2}{3Q^2}$$



4-point Function: HLbL tensor from HW2

C., Cata', D'Ambrosio, Greynat, Iyer (19), Leutgeb, Rebhan(19)



Propagators (from S_{YM})

(Massive) axial resonances

$$\underline{\underline{G_A^{\mu\nu}}}$$

5D axial Green function

$$G_A^{\mu\nu}(z, z'; q^2) =$$

$$G_A^T(z, z'; q^2) P_T^{\mu\nu}(q) + G_A^L(z, z'; q^2) P_L^{\mu\nu}(q)$$

$$P_T^{\mu\nu}(q) = \left(g^{\mu\nu} - \frac{q^\mu q^\nu}{q^2} \right),$$

$$P_L^{\mu\nu}(q) = \frac{q^\mu q^\nu}{q^2}$$

Pion propagator

$$\frac{\pi}{\underline{\underline{\frac{i}{q^2 - m_\pi^2}}}}$$

Pion and Massive axial resonances anomalous AVV vertices from S_{CS}



4-point Function: HLbL tensor from HW2 contn'd

$$\Pi^{\mu\nu\lambda\sigma} = \underbrace{\Pi_L^{(\pi, A)\mu\nu\lambda\sigma}}_{\text{pion \& massive axial reson.}} + \underbrace{\Pi_T^{(A)\mu\nu\lambda\sigma}}_{\text{massive axial reson.}}$$

where, for the massive resonances contributions

$$\begin{aligned} \Pi_{L,T}^{(A)\mu\nu\lambda\sigma} = & \underbrace{\left(g^{\mu\mu'} - \frac{q_1^\mu q_1^{\mu'}}{q_1^2} \right) \left(g^{\nu\nu'} - \frac{q_2^\nu q_2^{\nu'}}{q_2^2} \right) \left(g^{\lambda\lambda'} - \frac{q_3^\lambda q_3^{\lambda'}}{q_3^2} \right) \left(g^{\sigma\sigma'} - \frac{q_4^\sigma q_4^{\sigma'}}{q_4^2} \right)}_{\text{transverse projectors on external vector legs}} \\ & \times \underbrace{\varepsilon_{\mu'\nu'\alpha\beta} \varepsilon_{\lambda'\sigma'\gamma\delta}}_{\text{anomalous couplings}} \times \underbrace{P_{L,T}^{\alpha\gamma}}_{\text{L,T proj. in } G_A} \times \underbrace{A_{L,T}^{\beta\delta}}_{\text{z and z' integrals}} \end{aligned}$$

$A_{L,T}^{\beta\delta}$ contains combinations of the form $q_a^\beta q_c^\delta \mathcal{G}_A^{L,T}(q_a, q_b; q_c, q_d)$ with the convolution integrals

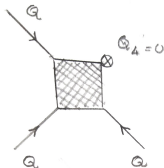
$$\mathcal{G}_A^L(q_a, q_b; q_c, q_d) = \int_0^{z_0} dz \int_0^{z_0} dz' v(z, q_a^2) \partial_z v(z, q_b^2) G_A^L(z, z') v(z', q_c^2) \partial_{z'} v(z', q_d^2)$$

$$\mathcal{G}_A^T(q_a, q_b; q_c, q_d) = \int_0^{z_0} dz \int_0^{z_0} dz' v(z, q_a^2) \partial_z v(z, q_b^2) G_A^T(z, z'; q_a+q_b) v(z', q_c^2) \partial_{z'} v(z', q_d^2)$$

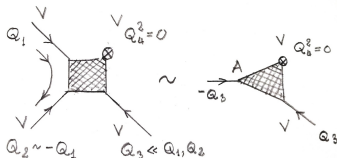
Short distance constraints

Two different kinematic limit Large Euclidean momenta in two different kinematic limits Quark loop and Melnikov-Vainshtein

Quark loop: $Q_1^2 \sim Q_2^2 \sim Q_3^2 \gg \Lambda_{QCD}^2$, $Q_4 = 0$



MV limit: $Q_1 \sim -Q_2$ and $Q_1^2 \sim Q_2^2 \gg Q_3^2 \gg \Lambda_{QCD}^2$



- ▶ **Quark loop:** For the longitudinal component of the HLbL tensor, the quark loop diagram in QCD gives:

$$\mathcal{W}_{12;34}^{\parallel} = -\frac{4}{9\pi^2 Q^4} \sim -\frac{0.44}{\pi^2 Q^4}. \quad (1)$$

This limit cannot be fulfilled by the pion contribution, which falls off like Q^{-6} . The relevant piece comes instead from the axial-vector tower:

$$\mathcal{W}_{12;34}^{\parallel} = -\frac{N_c}{3\pi^2 Q^4} \int_0^{\infty} x^4 K_1(x)^3 dx \sim -\frac{0.36}{\pi^2 Q^4}. \quad (2)$$

About 80% of the OPE coefficient. This mismatch could be due other hadronic contributions not included in our model (e.g., massive pseudoscalar mesons)

Short distance constraints cont'd

- **Melnikov-Veinshtein limit:** The key object is the product of two of the electromagnetic currents in the HLbL tensor

$$W^{\mu\nu}(q_1, q_2) = \int d^4x \int d^4y e^{i(q_1 \cdot x + q_2 \cdot y)} T \{ j_{\text{em}}^\mu(x), j_{\text{em}}^\nu(y) \}$$

In the kinematical limit $Q_1 = \xi Q - Q_3/2$; $Q_2 = -\xi Q - Q_3/2$ where ξ is large and all momenta are Euclidean. OPE gives:

$$\lim_{\xi \rightarrow \infty} W^{\mu\nu} = \frac{1}{\xi} \frac{2i}{Q^2} \epsilon^{\mu\nu\lambda\rho} Q_\lambda \sum_a \hat{d}^{a\gamma\gamma} \int d^4z e^{-iq_3 \cdot z} j_{5\rho}^{(a)}(z), j_{5\rho}^{(a)}(z) = \bar{q} \hat{Q}^2 \gamma_\rho \gamma_5 q$$

Thus, axial anomaly enters through the VVA 3-point function. The contribution of the **full axial-vector tower** is the relevant piece

$$J_{\perp}^{\sigma}(z, Q, Q_3) = -\frac{2Q^{\sigma}}{Q^2} a(z, Q_3) \left[\frac{1}{3} + \frac{1}{5} \left(\frac{Q_3}{Q} \right)^2 + \dots \right] \quad J_{\parallel}^{\sigma}(z, Q) = -\frac{2Q^{\sigma}}{3Q^2} \alpha(z).$$

The longitudinal piece is exact to all orders in Q_3 (anomaly non renormalization, correctly implemented in the model).

Cancellation between the pion and longitudinal axial-vector contributions in the chiral limit.

The pion contribution alone, i.e., $\omega_L^{(\pi)}(Q_3) \sim \frac{2N_c}{Q_3^2 + m_\pi^2} F_{\pi\gamma\gamma}(Q_3, 0)$, is clearly

incompatible with $\omega \sim Q_3^{-2}$ in the chiral limit.

No single particle exchange can saturate ω_L .

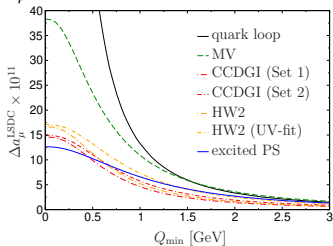
Relevance of the short distance constraints

Asymptotic behaviour of the HW2 4-point amplitude for large Euclidean momenta

- ▶ Main result: Melnikov-Vainshtein [Melnikov,Vainshtein(04)] QCD OPE constraints are satisfied by the sole contributions of pions and the whole tower of massive axial vectors. No contributions from other fields, at least in the chiral limit.
Pions dominate at low momenta, full tower of massive axial vector dominates for Large Euclidean momenta.
- ▶ In the literature the MV constraint
 - ▶ lead to an increase of the accepted estimate of the HLbL
 - ▶ was difficult to implement in other models:
For instance MV proposed a model with pointlike WZW at the vertex with physical photon, while [JegerlehnerNyffeler(09)] got the MV behaviour using LMD+V TFF's, with an elaborate choice of the parameters.
- ▶ the HW2 seems the first model to satisfy MV, without any of the above assumptions despite its simplicity
- ▶ axial anomaly plays a fundamental role in the MV constraint. Nothing similar for other SD constraints, such as the quark loop limit.

Pions and axial vectors contrib's: Numerical results

Help assessing SD corrections to a_μ^{HLbL} in White Paper



Estimates of the asymptotic behaviour (from White Paper), using different models

$a_\mu^{\text{HLbL}} \times 10^{10}$	$f_\pi / N_c = 31 \text{ MeV}$ $m_\rho = 776 \text{ MeV}$	$f_\pi = 93 \text{ MeV}$ $N_c = 3$
$a_\mu^{\text{PS}} (\pi^0 + \eta + \eta')$	8.1 (5.7+1.4+1.0)	11.2 (7.5+2.1+1.6)
$a_\mu^{\text{AL}} (a_1 + f_1 + f_1^*)$	1.4 (0.4+0.4+0.6)	1.4 (0.4+0.4+0.6)
$a_\mu^{\text{L}} (a_\mu^{\text{PS}} + a_\mu^{\text{AL}})$	9.6	12.6
$a_\mu^{\text{T}} (a_1 + f_1 + f_1^*)$	1.4 (0.4+0.4+0.6)	1.4 (0.4+0.4+0.6)
a_μ	11.0	14.0

Table: Results for the longitudinal and transverse contributions

Averaging out the results from the two sets of parameters and using the spread as an estimate of the uncertainty, our final number for the contribution of Goldstone modes and axial-vector states is

$$a_\mu^{\text{(AV+PS)}} = 12.5(1.5) \cdot 10^{-10}.$$

Scalars in HQCD: *non minimal* 5D Lagrangian

$$S_5 = \int d^5x \sqrt{g} (\mathcal{L}_{\text{YM}} + \mathcal{L}_{\text{CS}} + \mathcal{L}_X + \mathcal{L}'_X)$$

$$\mathcal{L}_{\text{YM}+\text{CS}} = -\lambda \text{tr} \left[F_{(L)}^{MN} F_{(L)MN} + F_{(R)}^{MN} F_{(R)MN} \right] + c \text{tr} [\omega_5(L) - \omega_5(R)]$$

$$\mathcal{L}_X = \rho \text{tr} \left[D^M X^\dagger D_M X - m_X^2 X^\dagger X - z \delta(z - z_0) V(X) \right]$$

$$\mathcal{L}'_X = \zeta_+ \text{tr} \left[X^\dagger X F_{(R)}^{MN} F_{(R)MN} + X X^\dagger F_{(L)}^{MN} F_{(L)MN} \right]$$

$$+ \zeta_- \text{tr} \left[X^\dagger F_{(L)}^{MN} X F_{(R)MN} \right].$$

- ▶ $V(X) = \frac{1}{2} \mu^2 \text{tr} [X^\dagger X] - \eta \text{tr} [(X^\dagger X)^2]$ is a scalar potential on the boundary, used it to enforce b.c. on the scalar field.
- ▶ If the scalar field has a non trivial profile $X_0(z)$, then \mathcal{L}'_X generates $s\gamma\gamma$ vertices from $X_0(z) X(x, z) F_{(V)}^{MN} F_{(V)MN}$, depending on the parameter $\zeta = \zeta_+ + \frac{1}{2} \zeta_-$.

HLbL tensor: One scalar exchange contribution

$$\begin{aligned}\Pi_{\mu\nu\lambda\rho}(q_1, q_2, q_3, q_4) &= \int_{\epsilon}^{z_0} dz \int_{\epsilon}^{z_0} dz' [T_{12}^{\mu\nu(a)} G^{(a)}(z, z'; s) T_{34}^{\lambda\rho(a)} \\ &\quad + T_{13}^{\mu\lambda(a)} G^{(a)}(z, z'; t) T_{24}^{\nu\rho(a)} + T_{14}^{\mu\rho(a)} G^{(a)}(z, z'; u) T_{23}^{\nu\lambda(a)}],\end{aligned}$$

where $s = (q_1 + q_2)^2$, $t = (q_1 + q_3)^2$, $u = (q_1 + q_4)^2$ and

$$T_{ij}^{\mu\nu(a)}(z) = \mathcal{P}_{ij}^{(a)}(z) P^{\mu\nu}(q_i, q_j) + \mathcal{Q}_{ij}^{(a)}(z) Q^{\mu\nu}(q_i, q_j),$$

where the two gauge-invariant tensors

$$P^{\mu\nu}(q_1, q_2) = q_2^\mu q_1^\nu - (q_1 \cdot q_2) \eta^{\mu\nu}$$

$$Q^{\mu\nu}(q_1, q_2) = q_2^2 q_1^\mu q_1^\nu + q_1^2 q_2^\mu q_2^\nu - (q_1 \cdot q_2) q_1^\mu q_2^\nu - q_2^2 q_1^2 \eta^{\mu\nu},$$

and the holographic form factors

$$\begin{aligned}\mathcal{P}_{ij}^{(a)}(z) &= 8\zeta \hat{d}^{a\gamma\gamma} \frac{X_0(z)}{z} v(z, q_i) v(z, q_j), \\ \mathcal{Q}_{ij}^{(a)}(z) &= 8\zeta \hat{d}^{a\gamma\gamma} \frac{X_0(z)}{z} \frac{\partial_z v(z, q_i)}{q_i^2} \frac{\partial_z v(z, q_j)}{q_j^2}.\end{aligned}\tag{3}$$

Numerical results for the scalars: Fixing the parameters

- ▶ Apparently scalar amplitudes do not completely comply with pQCD constraints (to be better understood)
- ▶ Our action has nine parameters: coefficients of bulk operators (λ , c , ρ , ζ_{\pm} , m_X), the size of the fifth dimension z_0 and the parameters of the scalar boundary potential (μ , η).
- ▶ For the scalar contributions to the HLbL, the only relevant are: ρ , z_0 , the combination $\zeta = \zeta_+ + \frac{1}{2}\zeta_-$, m_X , and the parameters of the boundary potential, which can be traded for the quark condensate $\langle \bar{q}q \rangle$ and γ .
- ▶ We required both UV and IR constraint on ζ and ρ to match $\langle SVV \rangle$ short-distance and the decay width of the lowest-lying scalars into two photons
- ▶ Flavour breaking, as we did in our paper for the Goldstone and axial-vector towers, generating copies of the original Lagrangian for each of the different light scalar states. Only γ , ρ and ζ , will be flavour-dependent.

Final results for the scalar contribution

- ▶ We have studied also the dependence of γ from the mass range (e.g. $m_\sigma = (450 - 550)$ MeV). Our estimate for the $\sigma(500)$ (certainly not a narrow resonance) contribution to the HLbL is

$$a_\mu^S(\sigma) = (-8.5 \pm 2.0) \cdot 10^{-11}$$

orientative, but should correctly captures the right order of magnitude for the uncertainty.

- ▶ The contributions of $a_0(980)$ and $f_0(990)$ can be computed in a less problematic way: both states are rather narrow.

$$a_\mu^S(a_0) = -0.29(13) \cdot 10^{-11}; \quad a_\mu^S(f_0) = -0.27(13) \cdot 10^{-11}$$

- ▶ Effect of higher massive states are found very small due to the peak of of kinematic kernels around 1 GeV

	$n = 1$	$n = 2$	Total
$a_\mu^S(\sigma)$	-8.5(2.0)	-0.07(2)	-8.7(2.0)
$a_\mu^S(a_0)$	-0.29(13)	-0.025(10)	-0.32(14)
$a_\mu^S(f_0)$	-0.27(13)	-0.025(9)	-0.29(14)
a_μ^S	-9(2)	-0.12(4)	-9(2)

Our final result is $a_\mu^S = -9(2) \cdot 10^{-11}$, rather close to previous estimates.

Conclusions

- ▶ HQCD model and in particular HW2 have been very effective in clarifying the role of vector and axial vector fields in fulfilling pQCD short distance constraints
- ▶ Thanks to the non renormalization properties of anomaly and the chiral formalism recovered in HW2, one has shown complete saturation of the MV constraint by axial vector resonances and pions, in the chiral limit
- ▶ These results have been useful to the theoretical community to help assessing the size of SD corrections to HLbL
- ▶ We have provided a HQCD estimate of the scalar contribution to the HLbL, including the $\sigma(500)$, $a_0(980)$ and $f_0(980)$ states together with an infinite tower of excited scalar states .
- ▶ In our final result $a_{\mu}^S = -9(2) \cdot 10^{-11}$, and we think that we have given conservative estimate for the uncertainty is given due mainly to the $\sigma(500)$ parameters. Adding to other contributions (e.g. pion and axial vectors) errors linearly, one would find aHLbL $a_{\mu} = 116(17) \cdot 10^{-11}$ which is in agreement with all the recent estimates of the HLbL.
- ▶ Note, however, the addition of scalar fields into the action, has some effect on the axial-vector, pion (and also massive pseudoscalars) and it calls for a more complete re-analysis. An understanding of some SD discrepancies of HQCD scalar amplitudes would be welcome too.

Back up slides

HLbL tensor: One scalar exchange contribution cont'd

Non vanishing dynamical coefficients for $(g - 2)$ from scalar exchange

$$\bar{\Pi}_3(Q_1, Q_2, \tau) = \int_{\epsilon}^{z_0} dz \int_{\epsilon}^{z_0} dz' \left[\mathcal{P}_{12}^{(a)} + (Q_1^2 + Q_2^2 + Q_1 Q_2 \tau) \mathcal{Q}_{12}^{(a)} \right] G_{(a)}(z, z'; s) \mathcal{P}_{34}^{(a)},$$

$$\bar{\Pi}_4(Q_1, Q_2, \tau) = \int_{\epsilon}^{z_0} dz \int_{\epsilon}^{z_0} dz' \left[\mathcal{P}_{13}^{(a)} + (Q_1^2 + Q_2^2 + Q_1 Q_2 \tau) \mathcal{Q}_{13}^{(a)} \right] G_{(a)}(z, z'; t) \mathcal{P}_{24}^{(a)},$$

$$\bar{\Pi}_8(Q_1, Q_2, \tau) = \int_{\epsilon}^{z_0} dz \int_{\epsilon}^{z_0} dz' \mathcal{P}_{14}^{(a)} G_{(a)}(z, z'; u) \mathcal{Q}_{23}^{(a)},$$

$$\bar{\Pi}_9(Q_1, Q_2, \tau) = \int_{\epsilon}^{z_0} dz \int_{\epsilon}^{z_0} dz' \mathcal{Q}_{12}^{(a)} G_{(a)}(z, z'; s) \mathcal{P}_{34}^{(a)}. \quad (4)$$

Scalar 3-point funct.: Asymptotic behaviour

$$\begin{aligned}\Gamma_{\mu\nu}^{(n,a)}(q_1, q_2) &= i \int d^4x e^{-iq_1 \cdot x} \langle 0 | T \{ j_{\text{em}}^\mu(x) j_{\text{em}}^\nu(0) \} | S_n^a \rangle \\ &= F_1^{(n,a)}(q_1^2, q_2^2) P_{\mu\nu}(q_1, q_2) + F_2^{(n,a)}(q_1^2, q_2^2) Q_{\mu\nu}(q_1, q_2),\end{aligned}$$

with transition form factors for each scalar meson:

$$\begin{aligned}F_1^{(n,a)}(q_1^2, q_2^2) &= 8\zeta \hat{d}^{a\gamma\gamma} \int_\epsilon^{z_0} dz \frac{X_0(z)}{z} \varphi_n^S(z) v_1(z) v_2(z), \\ F_2^{(n,a)}(q_1^2, q_2^2) &= 8\zeta \hat{d}^{a\gamma\gamma} \int_\epsilon^{z_0} dz \frac{X_0(z)}{z} \varphi_n^S(z) \frac{\partial_z v_1(z)}{q_1^2} \frac{\partial_z v_2(z)}{q_2^2}.\end{aligned}$$

The decay width of the scalar into two on-shell photons can be expressed in terms of $F_1^{(n,a)}(0, 0)$ alone as

$$\Gamma_{\gamma\gamma}^{(n,a)} = \frac{\pi\alpha^2}{4} m_n^3 \left| F_1^{(n,a)}(0, 0) \right|^2.$$

with

$$F_1^{(n,a)}(0, 0) = 8\zeta \hat{d}^{a\gamma\gamma} \int_\epsilon^{z_0} dz \frac{X_0(z)}{z} \varphi_n^S(z) = 8s_0 z_0^2 \zeta \hat{d}^{a\gamma\gamma} \frac{A_n}{\omega_n^2} [4J_3(\omega_n) - \omega_n J_4(\omega_n)]$$

Scalar 3-point funct.: Asymptotic behaviour cont'd

For highly virtual photons, *i.e.* for large Q , $v(z, Q) \sim QzK_1(Qz)$. In terms of the variables $Q^2 = \frac{1}{2}(Q_1^2 + Q_2^2)$ and $w = (Q_1^2 - Q_2^2)(Q_1^2 + Q_2^2)^{-1}$, such that $Q_{1,2} = Q\sqrt{1 \pm w}$ the model then predicts

$$\lim_{Q^2 \rightarrow \infty} F_1^{(n,a)}(Q_1^2, Q_2^2) = \frac{1536}{35} \zeta \hat{d}^{a\gamma\gamma} \frac{s_0}{z_0^4} \frac{A_n \omega_n}{Q^6} f_1(w),$$
$$\lim_{Q^2 \rightarrow \infty} F_2^{(n,a)}(Q_1^2, Q_2^2) = \frac{1152}{35} \zeta \hat{d}^{a\gamma\gamma} \frac{s_0}{z_0^4} \frac{A_n \omega_n}{Q^8} f_2(w),$$

with

$$f_1(w) = \frac{35}{384} \sqrt{1-w^2} \int_0^\infty dy y^7 K_1(y\sqrt{1+w}) K_1(y\sqrt{1-w})$$
$$= \frac{35}{32w^7} \left[30w - 26w^3 - 3(w^4 - 6w^2 + 5) \log\left(\frac{1+w}{1-w}\right) \right]$$
$$f_2(w) = \frac{35}{288} \int_0^\infty dy y^7 K_0(y\sqrt{1+w}) K_0(y\sqrt{1-w})$$
$$= \frac{35}{12w^7} \left[-15w + 4w^3 - \frac{9w^2 - 15}{2} \log\left(\frac{1+w}{1-w}\right) \right]$$

Notice that that the model does not match with pQCD, which predicts the asymptotic scalings

$$F_1(Q^2, Q^2) \sim Q^{-2}, \quad \text{and} \quad F_2(Q^2, Q^2) \sim Q^{-4}$$

and the identity $f_1(w) = f_2(w)$

Scalar 3-point funct. Asymptotic behaviour cont'd

The model however shows the right asymptotic pQCD scaling for the case of the $\langle SVV \rangle$ correlator

$$\begin{aligned}\Gamma_{\mu\nu}^{(a)}(q_1, q_2) &= i^2 \int d^4x \int d^4y e^{-i(q_1 \cdot x + q_2 \cdot y)} \langle 0 | T \{ j_{\text{em}}^\mu(x) j_{\text{em}}^\nu(y) j_S^3(0) \} | 0 \rangle \\ &= \bar{P}^{(a)}(q_1^2, q_2^2) P_{\mu\nu}(q_1, q_2) + \bar{Q}^{(a)}(q_1^2, q_2^2) Q_{\mu\nu}(q_1, q_2),\end{aligned}$$

- ▶ All momenta much larger than Λ_{QCD} , e.g. $q_1 = q_2 = q_3/2 \equiv q$

$$\lim_{q^2 \rightarrow \infty} \Gamma_{\mu\nu}^{(a)}(q, q) = \frac{16s_0\zeta}{z_0^3} \frac{\hat{d}^{a\gamma\gamma}}{Q^4} (q_\mu q_\nu - q^2 \eta_{\mu\nu}) \int_0^\infty dy y^6 K_1(2y) [K_1^2(y) - K_0^2(y)].$$

To be compared with the QCD OPE result

$$\lim_{q^2 \rightarrow \infty} \Gamma_{\mu\nu}^{(a)}(q, q) = 2\hat{d}^{a\gamma\gamma} \frac{\langle \bar{q}q \rangle}{Q^4} (q_\mu q_\nu - q^2 \eta_{\mu\nu}). \quad (5)$$

- ▶ Vector momenta hard and the scalar one soft. To leading order, $q_1 = -q_2 \equiv q$

$$\lim_{q^2 \rightarrow \infty} \Gamma_{\mu\nu}^{(a)}(q, -q) = \frac{64s_0\zeta}{15z_0^3} \frac{\hat{d}^{a\gamma\gamma}}{Q^4} (q_\mu q_\nu - q^2 \eta_{\mu\nu}) + \mathcal{O}(Q^{-6}). \quad (6)$$

Again, the scaling is the one expected from the OPE.